Simulation of ultrasonic beam propagation from phased arrays in anisotropic media using linearly phased multi-Gaussian beams

Anand, Chirag; Delrue, Steven; Jeong, Hyunjo; Shroff, Sonell; Groves, Roger M.; Benedictus, Rinze

DOI
10.1109/TUFFC.2019.2936106

Publication date
2020

Document Version
Final published version

Published in
IEEE Transactions on Ultrasonics, Ferroelectrics, and Frequency Control

Simulation of Ultrasonic Beam Propagation From Phased Arrays in Anisotropic Media Using Linearly Phased Multi-Gaussian Beams

Chirag Anand, Steven Delrue, Hyunjo Jeong, Sonell Shroff, Roger M. Groves, and Rinze Benedictus

***Abstract*— Phased array ultrasonic testing is widely used to test structures for flaws due to its ability to produce steered and focused beams. The inherent anisotropic nature of some materials, however, leads to skewing and distortion of the phased array beam and consequently measurement errors. To overcome this, a quantitative model of phased array beam propagation in such materials is required, so as to accurately model the skew and the distortion. The existing phased array beam models which are based on exact methods or numerical methods are computationally expensive or time consuming. This article proposes a modeling approach based on developing the linear phased multi-Gaussian beam (MGB) approach to model beam steering in anisotropic media. MGBs have the advantages of being computationally inexpensive and remaining non-singular. This article provides a comparison of the beam propagation modeled by the developed ordinary Gaussian beam and linear phased Gaussian beam models through transversely isotropic austenitic steel for different steering angles. It is shown that the linear phased Gaussian beam model outperforms the ordinary one, especially at steering angles higher than 20° in anisotropic solids. The proposed model allows us to model the beam propagation from phased arrays in both isotropic and anisotropic media in a way that is computationally inexpensive. As a further step, the developed model has been validated against a finite element model (FEM) computed using COMSOL Multiphysics.**

***Index Terms*— Anisotropy, beam modeling, multi-Gaussian, ultrasonic transducer arrays.**

I. Introduction

WHEN applying phased array ultrasonic non-destructive testing (NDT) in industry [1], [2], it is necessary to consider some challenges the generated ultrasonic beam is facing while propagating through anisotropic and layered materials. These challenges include beam skewing and beam diffraction due to anisotropy. Hence, this requires dedicated modeling of the phased array beam propagation as an integral part of an overall ultrasonic measurement model and also to understand the anisotropy effects and factor them in during practical applications. The differences between isotropic and anisotropic media are given in the following paragraph.

Isotropic homogeneous media are media in which the material properties are the same throughout the material and in all directions. Hence, in such materials, the velocity of the ultrasonic beam is independent of the direction of propagation. Anisotropic homogeneous materials have material properties which are direction dependent and hence the velocity of the propagating ultrasonic beam is also dependent on the direction of propagation.

Single transducer ultrasonic beam modeling has been performed by using different approaches. Some of the exact methods that exist require to model the transducer as a superposition of point sources [3] or to use the edge element method [4]. These methods become computationally expensive due to multiple integrals of high-frequency oscillations on the face of the transducer and at interfaces. Another method is to model the wavefield by a superposition of plane waves at the face of the transducer (angular spectrum) [5]–[7], as plane waves can be analytically transmitted and reflected from planar interfaces. Although this method can be used for anisotropic materials, it is not viable for curved interfaces as it leads to singularities. Other non-paraxial approximation methods apply numerical methods such as the finite element method (FEM) [8], [9] and the boundary element method (BEM) [10]. These numerical methods can be used for all complex interfaces and for anisotropic materials, but they become computationally very expensive, especially in the case where 3-D models are required. Some other methods for beam modeling, such as applying the full-wave methods by Green's solution to the dispersive wave equation [11], using nonlinear acoustics [12]–[17], etc., have been explored for isotropic homogeneous and inhomogeneous media, but have yet to be applied to layered anisotropic media. An alternative method which is based on paraxial approximation is to model the radiation as a superposition of Gaussian beams. As Gaussian beams are based on paraxial approximation, it has been shown that it is possible to analytically calculate the reflection and transmission of such beams at planar and curved interfaces [18]–[20]. Following this work, Huang [21] developed the multi-Gaussian beam (MGB) model for a single transducer to simulate propagation through an anisotropic medium. Following Huang's

Manuscript received January 10, 2019; accepted August 14, 2019. Date of publication August 19, 2019; date of current version December 26, 2019. *(Corresponding author: Chirag Anand.)*

C. Anand, R. M. Groves, and R. Benedictus are with the Faculty of Aerospace Engineering, Delft University of Technology, 2629 HS Delft, The Netherlands (e-mail: c.anand@tudelft.nl).

S. Delrue is with the Wave and Propagation Signal Processing Group, KU Leuven Kulak, 8500 Kortrijk, Belgium.

H. Jeong is with the Department of Mechanical Engineering, Wonkwang University, Iksan 54538, South Korea (e-mail: hjjeong@wku.ac.kr).

S. Shroff is with Clean Sky 2, 1060 Brussels, Belgium.

Digital Object Identifier 10.1109/TUFFC.2019.2936106

work, the MGB model for a single transducer was then applied to composite curved parts [22].

A phased array consists of multiple transducer elements to which time delays can be applied, allowing the steering of the ultrasonic beam in any desired direction or to focus the beam at a specific location. Beam steering and focusing of phased array transducers have been studied extensively by Azar *et al.* [23], which led to the formulation of time delay laws. To predict the wave field generated from arrays, single-element models such as the Rayleigh Sommerfeld have been expanded and used [24]. However, the exact and numerical models for multi-element transducers face the same drawbacks, as stated earlier for the single-element models. Kim *et al.* [25] generated the basis sets for rectangular-shaped array elements by applying intelligent use of the circ function. Park *et al.* [26] then expanded the MGB model to calculate the wave field from a phased array in isotropic materials. It was observed that beam steering above 20° was not accurately calculated as the beam is steered at an angle exceeding the paraxial limit of about 20°. To facilitate beam steering beyond the paraxial limit, an MGB model based on the application of linear phasing on the array element face was developed for wavefield simulation in isotropic structures by Huang *et al.* [27].

The application of anisotropic materials such as austenitic steel and carbon fiber-reinforced plastic (CFRP) in nuclear energy and aerospace industries has increased in the past few years. The NDT of such structures requires an understanding of wave propagation through anisotropic media. This has led to the expansion of the MGB model for a single-element transducer to include the effects of the slowness surface, which was then used to simulate the wave field in a graphite/epoxy composite [28]. As phased arrays are being used extensively for non-destructive inspection of such structures, it is also necessary to understand the beam propagation from arrays in such anisotropic structures.

The purpose of the current article is to combine the linear phasing method [27] with the MGB model for phased arrays in anisotropic media to calculate the ultrasonic beam propagation in anisotropic structures. Simulation results using both the ordinary MGB (OMGB) and the linearly phased MGB (LMGB) models for beam propagation through austenitic steel at different steering angles will be presented.

In Sections II and III, the theoretical basis of the OMGB and LMGB models for anisotropic media is described, starting from the MGB model for a single-element transducer and extending toward the models for phased array transducer radiation into anisotropic media. In Section IV, ultrasonic beam simulations in austenitic steel are compared using both the OMGB and LMGB models, and the results are verified by means of an FEM simulation in COMSOL Multiphysics. This article ends with conclusion in Section V.

II. Background Theory of the Paraxial MGB Model for Beam Propagation in Anisotropic Media

This section entails the preliminary theory of Gaussian beam propagation in anisotropic media. Consider a single circular transducer of diameter $2a$ with its emitting surface lying in the xy-plane and its normal pointing in the z-direction. The

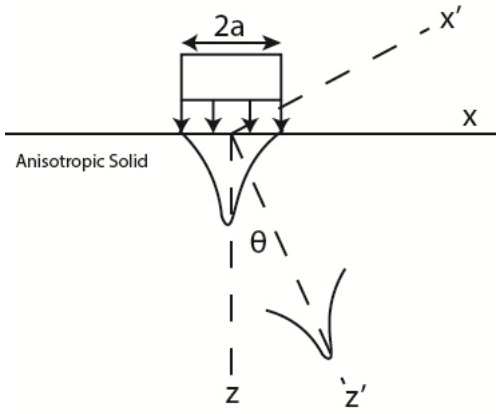

Fig. 1. Transducer radiating a Gaussian beam at an angle θ (group velocity direction).

z'-axis is taken along the group velocity direction (i.e., at an angle θ with respect to the normal direction z) and the $x'z'$-plane is taken as the plane of incidence as shown in Fig. 1.

Wen and Breazeale [19] determined that only ten Gaussian beam coefficients A_n and B_n were required to represent an ultrasonic beam. These coefficients were given in their seminal paper [19]. Using these coefficients, the velocity amplitude v and the phase $\mathbf{M}$ of a Gaussian beam in a solid can be described by the solution of the paraxial equation [21] as

$$\boldsymbol{v}=v_0\sum_{n=1}^{10}A_n\frac{\sqrt{\det[\mathbf{M}(z')]}}{\sqrt{\det[\mathbf{M}(0)]}}\mathbf{d}\exp\left[i\omega\left(\frac{z'}{u_p}+\frac{1}{2}\mathbf{X}^T\mathbf{M}(z')\mathbf{X}\right)\right] \tag{1}$$

with

$$\mathbf{M}(0)_n=\frac{2\,iB_n}{\omega a^2},\mathbf{M}(z')=\mathbf{M}(0)\left[\mathbf{I}+\frac{D}{c_p}\mathbf{s}_p\mathbf{M}(0)\right]^{-1} \tag{2}$$

and

$$\mathbf{s}_p=c_p\begin{bmatrix}(c_p-2C) & -D\\ -D & (c_p-2E)\end{bmatrix}. \tag{3}$$

In (1) and (2), v_0 and $\mathbf{M}(0)$ are the initial velocity and phase amplitudes at the transducer face, $\mathbf{X}(x',\ y',\ z')$ are the coordinates in the group velocity direction, and $\mathbf{d}$ is the polarization vector. $\mathbf{I}$ is the identity matrix, ω is the angular frequency, and c_p and u_p are the magnitudes of the phase velocity and group velocity, respectively. The parameters C, D, and E in (2) and (3) are the slowness surface curvatures, which are measured in the slowness coordinates. They determine the rate of divergence or convergence of the beam due to diffraction. These parameters are obtained by expanding the z′ component of the slowness vector s_0 using a Taylor series expansion as follows:

$$s_{z'}=s_0+As_{x'}+Bs_{y'}+\left(C-\frac{1}{2s_0}\right)s_{x'}^2+Ds_{x'}s_{y'}+\left(E-\frac{1}{2s_0}\right)s_{y'}^2 \tag{4}$$

where $s_{x'}$, $s_{y'}$, and $s_{z'}$ are the slowness vector components and s_0 is the slowness value. Expansion of the slowness vector also gives the parameters A and B which are related to the deviation or skew of the group velocity

from the slowness direction. For an isotropic material, $A = B = C = D = E = 0$.

In practical applications, transducer arrays mainly consist of rectangular-shaped elements of a fixed length and width. Hence, in Section III, (1) is modified for transducer arrays with rectangular-shaped elements.

III. Ordinary and Linearly Phased MGB Models for Phased Array Beam Propagation in Anisotropic Media

A. Development of the OMGB Model for Phased Arrays

The first model developed in this article to calculate the ultrasonic beam propagation from an array of transducers in anisotropic media is based on the expanded MGB model developed for an array of rectangular transducers [26], [29] in isotropic media. First, this expanded MGB model for element j developed for isotropic media is shown below

$$\mathbf{v}_j = \mathbf{d}\exp\left(i\omega\frac{z}{c_p}\right) \sum_{m=1}^{10}\sum_{n=1}^{10} v_0 \frac{A_n A_m}{\sqrt{1+c_p z[\mathbf{M}_{mn}(0)]_{11}}\sqrt{1+c_p z[\mathbf{M}_{mn}(0)]_{22}}} \times \exp\left[\frac{1}{2}\mathbf{X}^{\mathrm{T}}\mathbf{M}_{mn}(z)\mathbf{X}\right] \tag{5}$$

where

$$[\mathbf{M}_{mn}(0)]_{11} = \frac{iB_m}{D_1}, \quad [\mathbf{M}_{mn}(0)]_{22} = \frac{iB_n}{D_2}$$
$$D_1 = \frac{k_p a_1^2}{2}, \quad D_2 = \frac{k_p a_2^2}{2} \tag{6}$$
$$[\mathbf{M}_{mn}(z)]_{11} = \frac{[\mathbf{M}_{mn}(0)]_{11}}{1+c_p z[\mathbf{M}_{mn}(0)]_{11}}$$
$$[\mathbf{M}_{mn}(z)]_{22} = \frac{[\mathbf{M}_{mn}(0)]_{22}}{1+c_p z[\mathbf{M}_{mn}(0)]_{22}}$$
$$[\mathbf{M}_{mn}(z)]_{12} = [\mathbf{M}_{mn}(z)]_{21} = 0. \tag{7}$$

The subscripts in (7) are the indices for matrix elements. For isotropic materials, the group velocity and the phase velocity are equal, hence in (5) the phase velocity c_p is used. k_p is the wavenumber and a_1 and a_2 are the width and the length of the rectangular transducer, respectively. A_n, A_m, B_n, and B_m are the Wen and Breazzle coefficients as stated before.

Now, in this article, the OMBG for anisotropic media is developed by modifying (5) using parameters from and by using some simple linear algebra and matrix rearrangement.

The OMGB model for the array in anisotropic media is formulated as shown below, where now the angle of incidence is in the group velocity direction, hence the rotated coordinates are now $\mathbf{X}'(x', y', z')$:

$$\mathbf{v}_j = \mathbf{d}\exp\left(i\omega\frac{z'}{u_p}\right)\sum_{m=1}^{10}\sum_{n=1}^{10} v_0 A_n A_m \frac{\sqrt{\det[\mathbf{M}_{mn}(z')]}}{\sqrt{\det[\mathbf{M}_{mn}(0)]}} \times \exp\left[\frac{1}{2}\mathbf{X}'^{\mathrm{T}}\mathbf{M}_{mn}(z')\mathbf{X}'\right]. \tag{8}$$

For anisotropic media, $\mathbf{M}_{mn}(z')$ is modified as

$$\mathbf{M}_{mn}(z') = \mathbf{M}_{mn}(0)\left[\boldsymbol{I} + \frac{D}{c_p}\boldsymbol{S}_p\boldsymbol{M}_{mn}(0)\right]^{-1}. \tag{9}$$

The normalized velocity field from an array of transducers can be then given as follows:

$$\mathbf{v} = \sum_{j=1}^{N}\mathbf{v}_j \exp(i\omega t_j) \tag{10}$$

where t_j is the time delay applied to the jth array element to focus and steer the beam and v_j is the normalized velocity field of a single element.

For both focusing and steering the beam, the time delay t_j to be applied is given by [24]

$$t_j = \frac{F}{c_p}\left\{\begin{array}{l}\left[1+\left(\frac{\overline{N}d}{F}\right)^2 + \frac{2\overline{N}d}{F}\sin\theta_j\right]^{1/2} \\ -\left[1+\left(\frac{(j-\overline{N})d}{F}\right)^2 + \frac{2(j-\overline{N})d}{F}\sin\theta_j\right]^{1/2}\end{array}\right\}. \tag{11}$$

Here, F is the focus distance, d is the pitch of the element, $\overline{N} = (N-1)/2$ where N is the number of elements, and θ_j is the steering angle of each element.

In anisotropic media, it is important to have accurate angles of propagation from the element to the desired point as the velocity used to calculate the time delays is dependent on the angle of propagation of the beam. Using the ray theory [30] and tracing the ray from element j to the desired point at a distance F and angle θ_j, we calculate the phase velocity along this ray. Using this calculated phase velocity, we then apply the accurate time delay to the element.

As has been observed in the work done by Park *et al.* [26], the OMGB model fails when the beam is steered above 20° in isotropic media. It is shown later in this article that the same behavior is observed in anisotropic media. To solve this problem, a linear phasing is applied to the array elements, as shown in Section IV. The LMGB beam model is then modified to simulate phased array ultrasonic beams in anisotropic structures.

B. Development of LMGB From an Array Into Anisotropic Media

Huang *et al.* [27] showed that by introducing a continuous, linearly varying phase on the face of the transducer, a steered sound beam can be produced from a virtual transducer which has its axis in the steering direction. They also showed that the phasing of a Gaussian beam would shift it to a steering direction which is still within the paraxial limit.

The nonparaxial expansion given by Zhao and Gang [31], though appropriate for a single-layered isotropic medium, is not suitable for a multi-layered anisotropic medium due to the fact that the formulation does not support the formation of **M** matrices which reduce the complexity when dealing with a multi-layered anisotropic medium. When dealing with layered media, the **M** matrices can be further decomposed into A, B, C, and D matrices which make beam radiation calculation in layered media simpler.

Hence, the linear phasing on the face of the transducer can be applied by rotating the coordinates in the required

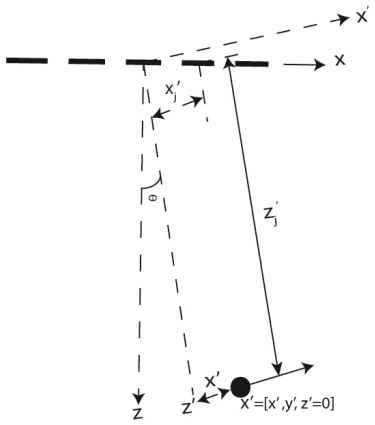

Fig. 2. Rotated coordinates in the steering direction.

steering direction from the central axis of the array θ as shown in Fig. 2.

Doing so, the coordinates and the $\mathbf{M}(0)$ matrix have to be modified to simulate the linear phasing over each element. The velocity also has to be multiplied by an amplitude correction factor $(1/\cos\theta_j)$, as shown in the following equation. Because of the anisotropic nature of the material, θ_j has to be calculated separately for each element using ray theory. It might be added here that θ_j corresponds to the steering angle from element j, whereas θ corresponds to the steering angle from the center of the array

$$v'_j(x', y', z') = \frac{1}{\cos\theta_j} v_j \begin{pmatrix} x \to x', y \to y', z \to z', d \to d' \\ \mathbf{M}(0) \to \dfrac{1}{\cos^2\theta_j}\mathbf{M}(0) \end{pmatrix}. \tag{12}$$

Using the OMGB model for a phased array in anisotropic media and modifying it to including the amplitude correction factor and the modified phase, the velocity field for the jth element is given as

$$\mathbf{v}_j = \exp(ikz')d' \sum_{m=1}^{10}\sum_{n=1}^{10} \frac{A_n A_m}{\sqrt{1+\frac{c_p}{u_p}z'[\mathbf{M}_{mn}(0)]_{11}}\sqrt{1+\frac{c_p}{u_p}z'[\mathbf{M}_{mn}(0)]_{22}}} \times \exp\left(\frac{i\omega}{2}\mathbf{X}'^{\mathrm{T}}\mathbf{M}_{mn}(z')\mathbf{X}'\right) \tag{13}$$

where

$$[\mathbf{M}_{mn}(z)']_{11} = \frac{[\mathbf{M}_{mn}(0)]_{11}}{1+z'\frac{c_p}{u_p}(c_p - 2\ C)[\mathbf{M}_{mn}(0)]_{11}} \tag{14}$$

$$[\mathbf{M}_{mn}(z)']_{22} = \frac{[\mathbf{M}_{mn}(0)]_{22}}{1+z'\frac{c_p}{u_p}(c_p - 2\ E)[\mathbf{M}_{mn}(0)]_{22}}$$

$$\mathbf{X}'_j = \begin{bmatrix} x' & y' \end{bmatrix}. \tag{15}$$

Directivity of the element also plays an important role in an array. The directivity for each element [24] is given as

$$D_r = \frac{\sin[(k_p a_1 \sin\theta_j)/2]}{(k_p a_1 \sin\theta_j)/2} \tag{16}$$

where k_p is the wavenumber.

The directivity can then be included in (13) as follows:

$$\mathbf{v}'_j = D_r \exp(ikz')d' \sum_{m=1}^{10}\sum_{n=1}^{10} \frac{A_n}{\sqrt{1+\frac{c_p}{u_p}z'[\mathbf{M}_{mn}(0)]_{11}}} \times \frac{A_m}{\sqrt{1+\frac{c_p}{u_p}z'[\mathbf{M}_{mn}(0)]_{22}}} \times \exp\left(\frac{i\omega}{2}\mathbf{X}'^{\mathrm{T}}_j\mathbf{M}_{mn}(z')\mathbf{X}'_j\right). \tag{17}$$

Section III-C presents details on how the FEM simulation was carried out.

C. Development of the FEM Model Using COMSOL

The numerical model was computed using commercially available FEM software COMSOL Multiphysics. An implicit solver is used to solve this problem. The construction of the FEM model in COMSOL comprises the following steps.

1) *Construction of Geometry:* For verifying the model at hand, it consists of a 2-D rectangular domain representing an anisotropic material with a number of line elements at the upper boundary which represent the array elements.
2) *Definition of the Domain and the Boundary Conditions:* For the domain, this consists of the definition of material properties (density and elastic tensor). A boundary force is applied on the array elements. These take into account the time delays to be applied to focus and steer the beam. For the other boundaries, perfectly matching layers (PMLs) are defined to model an infinitely large domain so as to reduce the reflections from the boundaries.
3) The computational region has to be discretized into smaller elements (i.e., mesh elements) on which the solutions will be calculated. For this problem, quadratic triangular Lagrange elements are chosen. For ultrasonic propagation problems, it is recommended that the element size should be lesser than $\lambda/6$, where λ is the wavelength [32].
4) *Postprocessing of the Output:* The model output is then postprocessed to remove the shear wave contributions. This is done by using a spatial Fourier transform to identify the wavenumber of the shear waves and the longitudinal waves. The shear wave contribution is then filtered out and an inverse Fourier transform returns only the longitudinal wave contribution in the beam.

For this article, the COMSOL model consisted of a rectangular domain of 80 mm × 100 mm with mesh elements of the size of $\lambda/7$. The PMLs of dimensions 100 mm × 20 mm are defined at the boundaries of the rectangular domain. The domain material properties are user-defined, as shown in Table I.

Fig. 3 shows an example where the beam is steered at an angle of 20°. In Fig. 3(a), the wavefield consists of both quasi-longitudinal and quasi-shear waves. Fig. 3(b) shows the wavenumbers present, where k_x is the wavenumber component in the x-direction and k_z is the wavenumber component in the z-direction. The lower k_z corresponds to the quasi-longitudinal

TABLE I
MATERIAL PROPERTIES

Material properties	Value
C_{11}=C_{22}	241.10 GPa
C_{33}	240.12 GPa
C_{12}	96.92 GPa
C_{13}=C_{23}	138.03 GPa
C_{44}=C_{55}	112.29 GPa
C_{66}	72.09 GPa
Density (ρ)	7820 kg/m^3

wave. Fig. 3(c) shows the wavefield after filtering out the shear wave contribution. The beam field now consists of the quasi-longitudinal wave.

IV. SIMULATION RESULTS

In this section, we present results simulated by the OMGB and LMGB models for linear phased arrays in anisotropic materials. These models were programed and executed using MATLAB 2016. These results are also verified by comparing them to the results obtained by a numerical FEM implemented in the commercially available software package COMSOL Multiphysics. The anisotropic material considered here is austenitic steel (transversely isotropic) with the following elastic constants [10].

The phased array ultrasonic transducer modeled consists of 32 elements, with an element pitch of 0.49 mm, an element width of 0.49 mm, and a center frequency of 2.25 MHz. The beam profile is computed to a depth of 80 mm in the solid and with a desired beam focus F at 40 mm.

In the following sections, we will first illustrate the beam distortion effects for specific materials. Next, we will compare the OMGB and LMGB models for angles below the paraxial restriction, and after that, we will present the comparison and verification of the LMGB model for angles above the paraxial restriction.

A. Effect of Slowness Surface Curvatures on the Beam

Fig. 4 shows the slowness surfaces of austenitic steel for quasi-longitudinal (qp), quasi-shear horizontal (qsh), and quasi-shear vertical (qsv) waves [see Fig. 4(a)], as well as the variation of the C and E parameters [see Fig. 4(b)] and the beam skew [see Fig. 4(c)].

To show the effect of the slowness parameters on the beam propagation, the values are artificially varied from $C = E = 0$ (isotropic case) to $C = E = -4.9$ mm/μs. Beam profiles are obtained using the OMGB model for 0° propagation and are

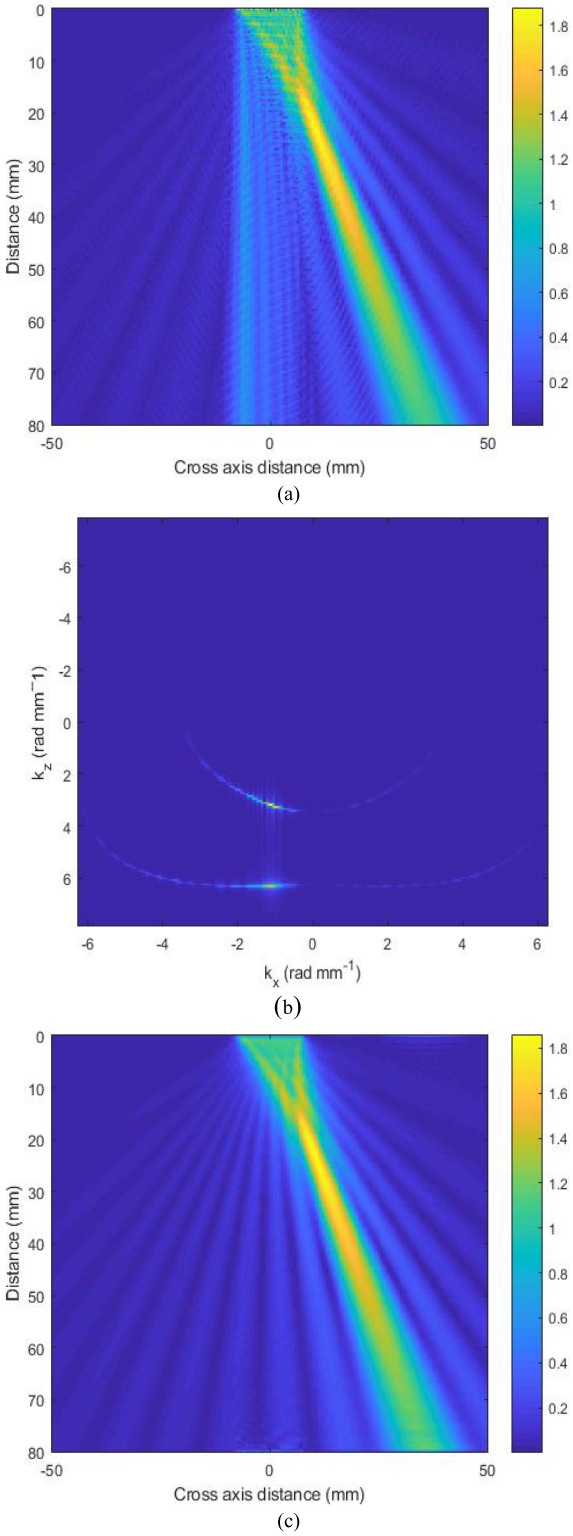

Fig. 3. (a) Beam field with quasi-longitudinal and quasi-shear waves. (b) Wave numbers corresponding to quasi-longitudinal and quasi-shear waves. (c) Beam field consisting of only quasi-longitudinal waves.

shown with the corresponding curvature values in Fig. 5. The desired focus F is 40 mm and the steering angle θ is 0°. It can be seen that as the curvature values move toward 0, the beam extends, whereas for larger negative curvature values, the beam moves toward the face of the transducer (compression).

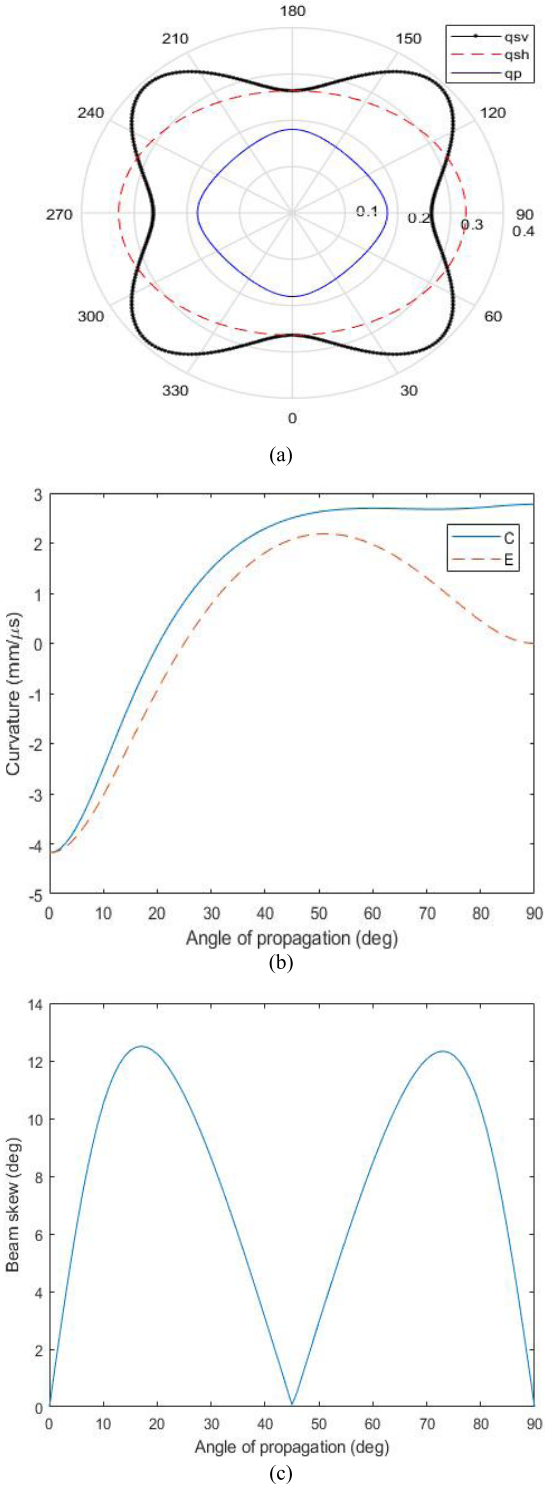

Fig. 4. Beam field using (a) slowness surfaces, (b) slowness surface curvatures C and E, and (c) beam skew.

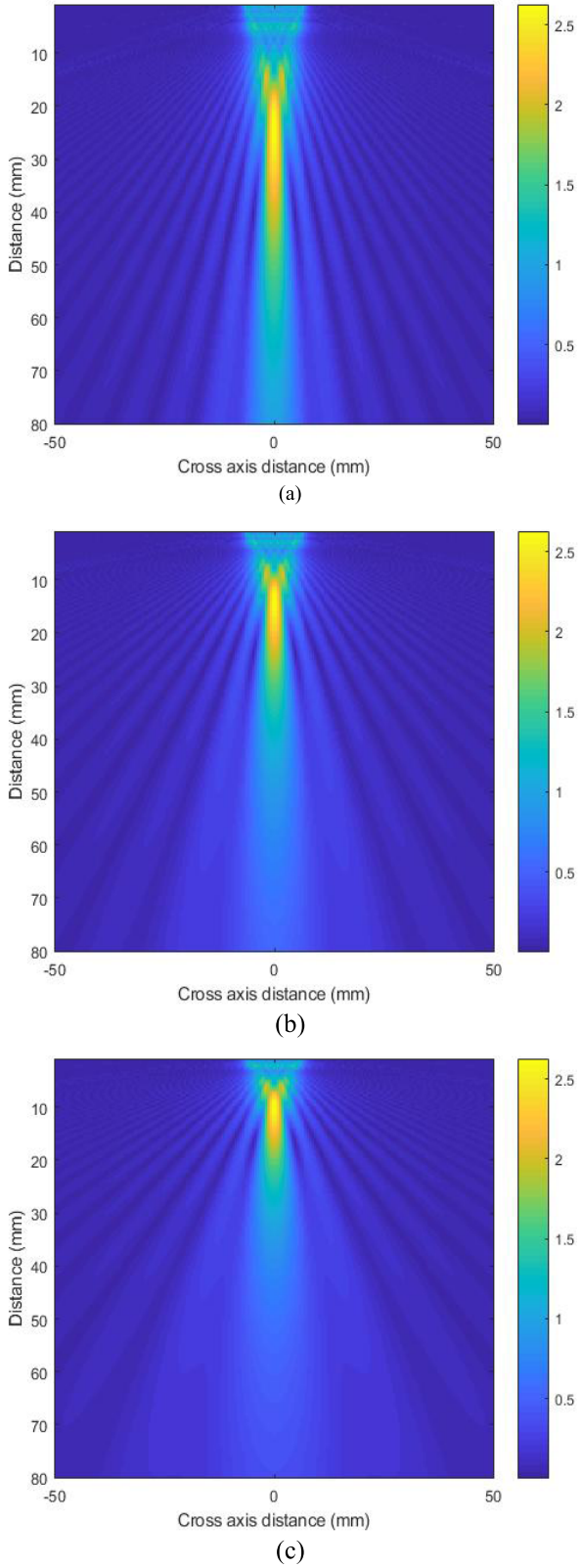

Fig. 5. Beam field: (a) $C = E = 0$, (b) $C = E = -2.5$ mm/μs, and (c) $C = E = -4.9$ mm/μs.

B. Comparison of the OMGB and LMGB Models Below the Paraxial Limit

Figs. 6 and 7 show the comparison between the OMGB and LMGB models steered at an angle of 0° and 10°, respectively, and focused at 40 mm. As can be seen in Figs. 6 and 7, both the LMGB and OMGB models are approximately the same for angles below 20°. The slowness curvature values for the steering angle 0° are $C = E = -4.18$ mm/μs and for the steering angle 10° are $C = -2.4856$ mm/μs and $E = -3.0292$ mm/μs.

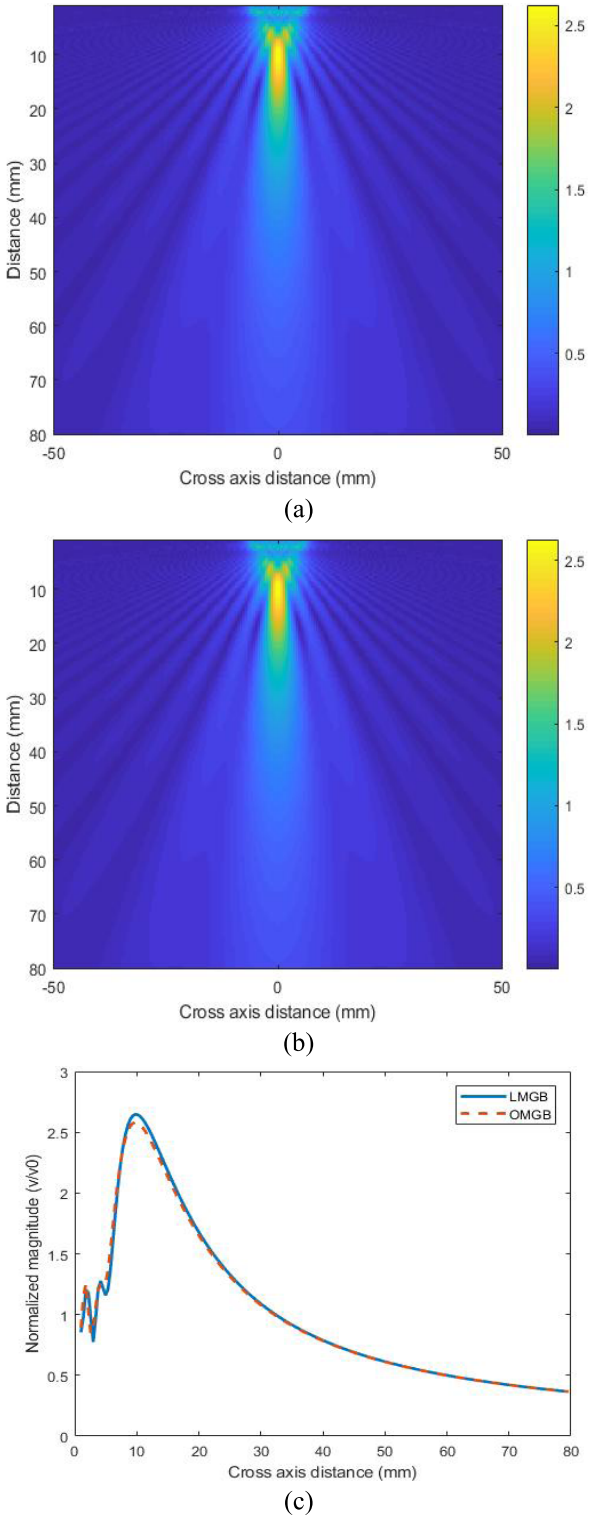

Fig. 6. Beam field at a steering angle of 0° using (a) OMGB, (b) LMGB, and (c) on-axis magnitude.

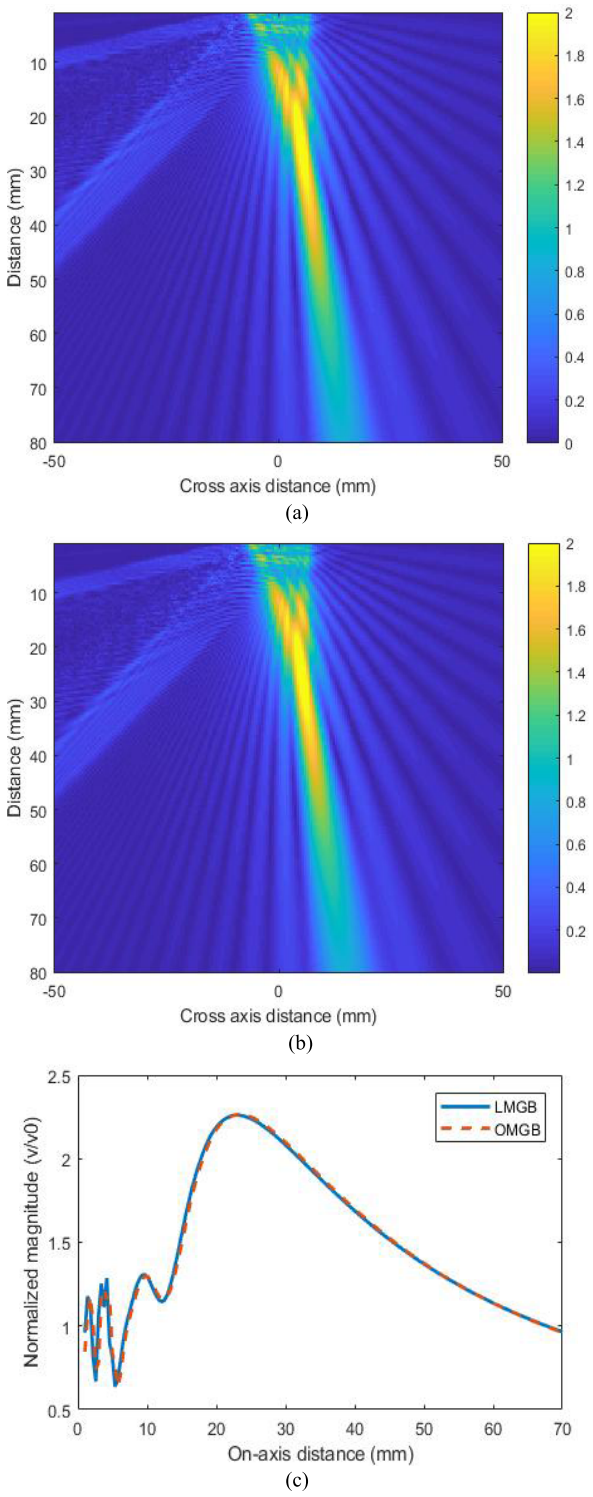

Fig. 7. Beam field at a steering angle of 10° using (a) OMGB, (b) LMGB, and (c) on-axis magnitude.

C. Comparison of OMGB, LMGB, and FEM Models Above the Paraxial Limit

Fig. 8(a)–(c) shows the beam propagation calculated using COMSOL, LMGB, and OMGB models, respectively, when the beam is steered at an angle of 30° with slowness curvature values, $C = 1.4888$ mm/μs and $E = 0.7769$ mm/μs. As can be seen in the figures, the shape and the structure of the beam are maintained for the COMSOL and LMGB cases, whereas it breaks down for the OMGB model. Fig. 9(a)–(c) shows the on-axis pressure calculated by the three modeling techniques for steering angles 20°, 30°, and 45°, respectively. It can be seen that at higher steering angles, the on-axis magnitude calculated using the OMGB model is drastically different from the LMGB and COMSOL models. Fig.10(a)–(c) shows the

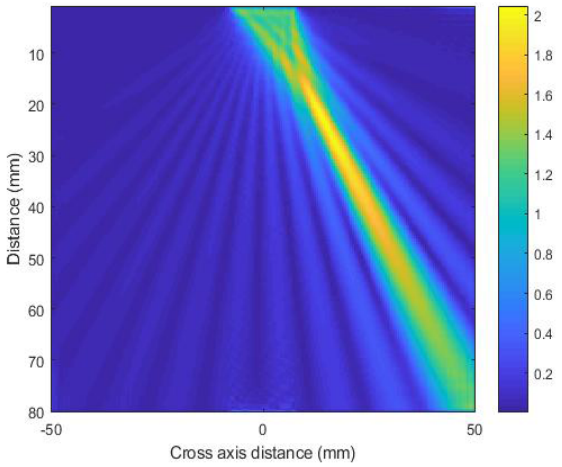

(a)

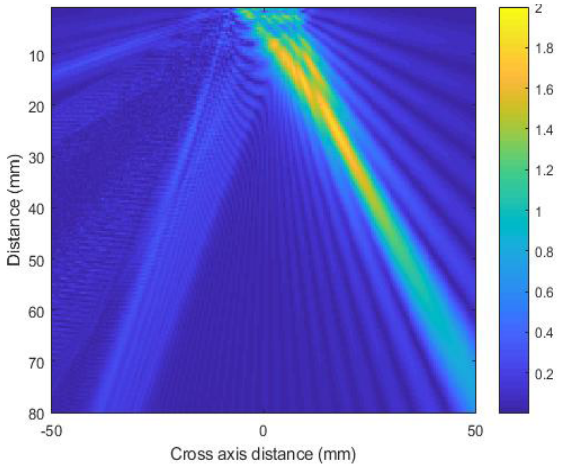

(b)

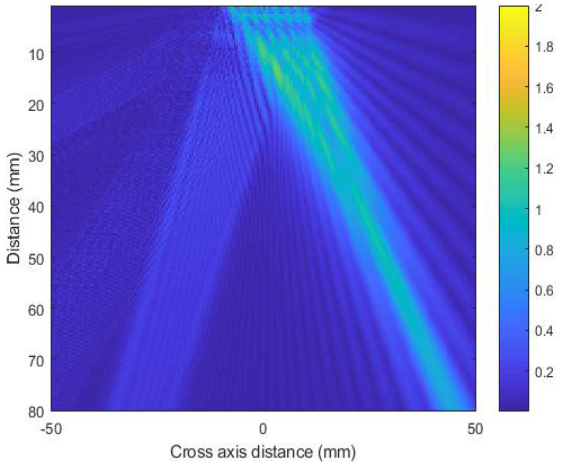

(c)

Fig. 8. Beam field using (a) COMSOL, (b) LMGB, and (c) OMGB for a steering angle of 30°.

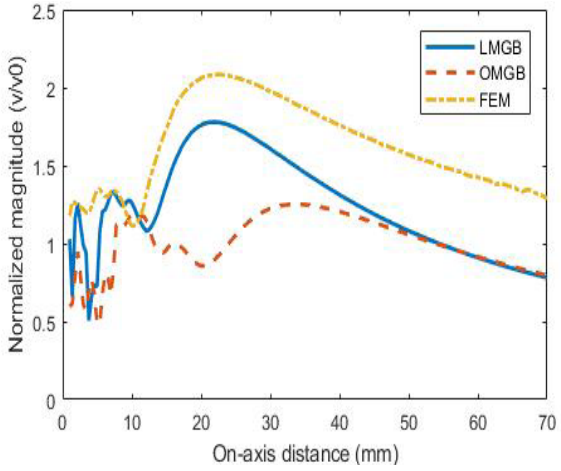

(a)

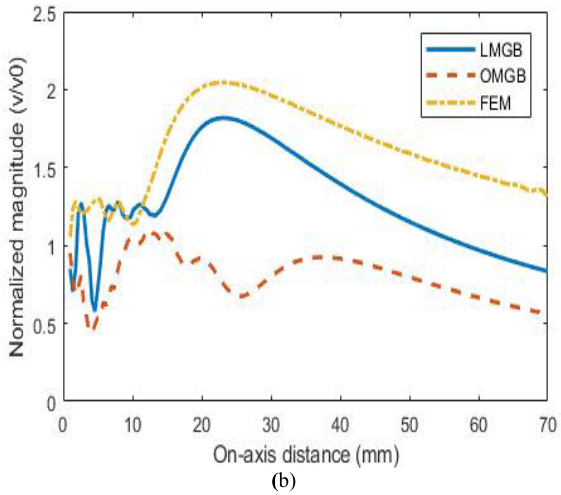

(b)

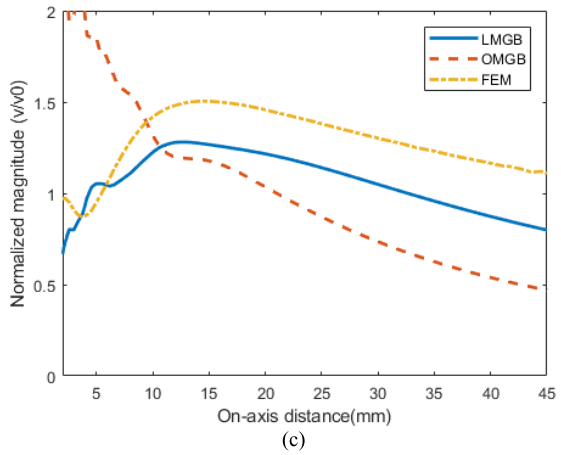

(c)

Fig. 9. On-axis beam fields calculated using the analytical and numerical models for the steering angles of (a) 20°, (b) 30°, and (c) 45°.

on-axis pressure calculated by the three modeling techniques for steering angles 20°, 30°, and 45°, respectively, in the decibel scale (dB). Fig. 11 shows a comparison between the LMGB and OMGB models for different angles at different on-axis distances in the dB scale. It is observed that as the angle of propagation increases, the relative error in the far-field increases.

V. Discussion

It is seen from Fig. 8 that the shape and the structure of the beam remain intact for both the numerical (COMSOL) and LMGB models, whereas the beam loses its shape and structure when computed using the OMGB model. This is attributed to the beam from the array elements not being in the paraxial limit. The linear phasing applied to the elements in the LMGB model shifts the axis for each element in the steered direction,

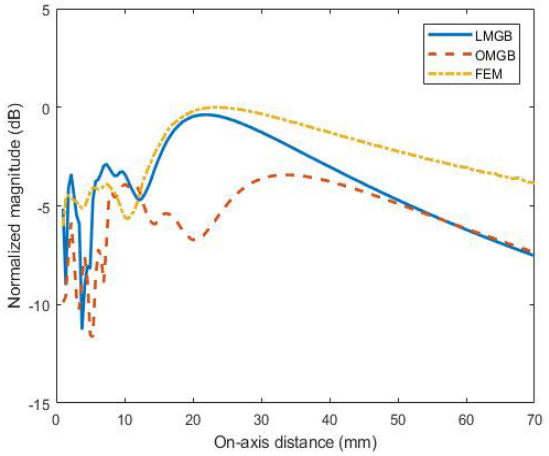

(a)

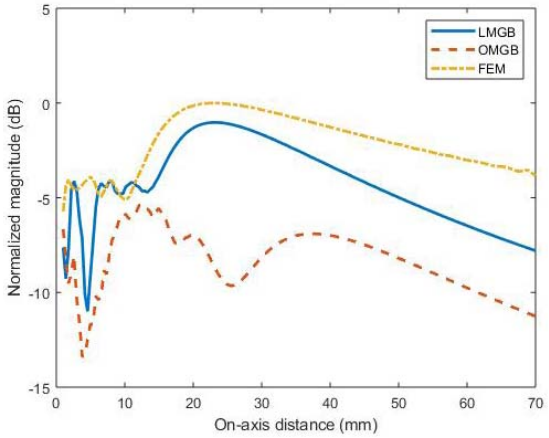

(b)

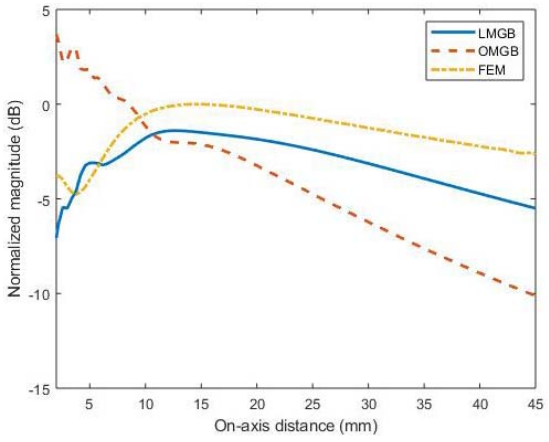

(c)

Fig. 10. On-axis beam fields calculated using the analytical and numerical models for the steering angles of (a) 20°, (b) 30°, and (c) 45° in the decibel (dB) scale.

hence maintaining the paraxial limit in the steering direction. It is also noted that the magnitude curve for FEM falls slower than that using analytical models, hence the beam appears to extend for a longer distance. Two factors have been attributed to this: 1) the array elements used in the analytical models have finite lengths and widths, whereas in the COMSOL simulation though the array elements have a finite width, their lengths are relatively infinite affecting the beam extension and 2)

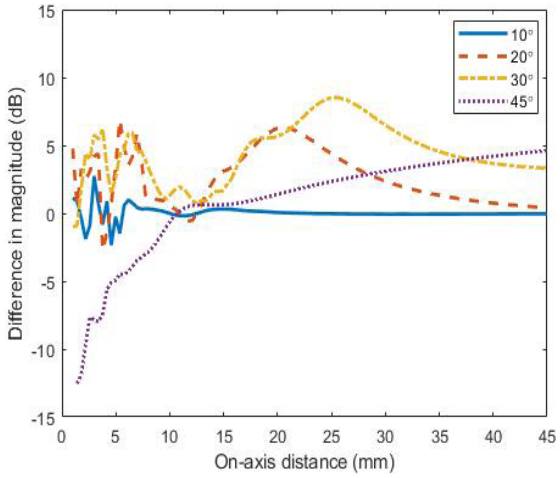

Fig. 11. Difference in on-axis amplitudes (dB) for different steering angles between the LMGB and OMGB models.

the slowness surface curvatures control the beam diffraction effects, and these curvature values are approximates found by fitting a second-order polynomial. Using higher order polynomials might give more accurate slowness curvature values eliminating this discrepancy too. While comparing the normalized magnitude of the on-axis pressure of the three models, it is seen that the COMSOL and LMGB models show the same shape and structures with an error of ± 1 dB, as seen from Fig. 10 of the maximum magnitude, in contrast to the OMGB model. The slight discrepancy in the normalized magnitude in the COMSOL and LMGB models is attributed to the fact that the normalization depends on the magnitude at the surface of the elements which might differ using both the approaches as it is in the near field of the beam.

It is also seen from Fig. 4 that the C and E slowness parameters control the beam diffraction. The beam is seen to move toward the transducer (compression) when the slowness values are varied from 0 to -4.9 mm/μs. Hence, for austenitic steel, even though the focus required is 40 mm, the beam moves toward the transducer with a focus at 15 mm. This is consistent with the anisotropy factor AF [33] as shown below:

$$\mathrm{AF} = \frac{C_{44}}{C_{33}} + \frac{(C_{13} + C_{44})^2}{C_{33}(C_{33} - C_{44})}. \tag{18}$$

For an isotropic material, AF is unity, whereas for austenitic steel, it is 2.51. This means that traveling along the z-axis in the austenitic steel, the equivalent distance that the beam has to travel in an isotropic material to achieve the same diffraction is $2.51z$.

Fig. 3(c) shows the beam skew angles, but by applying the time delays, it is seen from Figs. 7 and 8 that the skewing can be overcome.

At this point, it can also be noted that though the numerical model was able to predict the beam propagation, a relatively larger amount of computational resources and time as compared to the MGB models were required to compute it. The LMGB/OMGB models took 180 s on a personal computer with 8 GB of RAM, whereas the COMSOL model took 400 s on a computer with 32 GB of RAM. Also,

restrictions were placed on the highest frequency which can be modeled.

VI. Conclusion

This article proposes a modeling approach for anisotropic media using phased arrays to optimize the inspection of such structures. The modeling approach uses the LMGB model to calculate the beam fields in anisotropic media. Comparisons between the OMGB model and the LMGB model, and as verified by a numerical model, show that the LMGB model is able to predict beam fields successfully even when the beam is steered above 20°. It is also seen that owing to the anisotropic nature of the material, beam compression takes place due to which the location of the focal point also changes. Beam skewing is also observed due to the anisotropic nature of the material which is compensated by calculating the appropriate time delays.

References

[1] J. C. Somer, "Electronic sector scanning for ultrasonic diagnosis," *Ultrasonics*, vol. 6, no. 3, pp. 153–159, 1968.

[2] B. W. Drinkwater and P. D. Wilcox, "Ultrasonic arrays for non-destructive evaluation: A review," *NDT E Int.*, vol. 39, no. 7, pp. 525–541, Oct. 2006.

[3] L. W. Schmerr, Jr., *Fundamentals of Ultrasonic Nondestructive Evaluation: A Modeling Approach*, 2nd ed. Springer, 2016.

[4] T. P. Lerch, L. W. Schmerr, and A. Sedov, "Ultrasonic beam models: An edge element approach," *J. Acoust. Soc. Amer.*, vol. 104, no. 3, pp. 1256–1265, 1998.

[5] J. W. Goodman, *Introduction to Fourier Optics*, vol. 8, no. 5, 2nd ed. New York, NY, USA: McGraw-Hill, 1996.

[6] D. Belgroune, J. F. De Belleval, and H. Djelouah, "Modelling of the ultrasonic field by the angular spectrum method in presence of interface," *Ultrasonics*, vol. 40, nos. 1–8, pp. 297–302, 2002.

[7] M. E. Schafer and P. A. Lewin, "Transducer characterization using the angular spectrum method," *J. Acoust. Soc. Amer.*, vol. 85, no. 5, pp. 2202–2214, 1989.

[8] Z. You, M. Lusk, R. Ludwig, and W. Lord, "Numerical simulation of ultrasonic wave propagation in anisotropic and attenuative solid materials," *IEEE Trans. Ultrason., Ferroelectr., Freq. Control*, vol. 38, no. 5, pp. 436–445, Sep. 1991.

[9] W. Lord, R. Ludwig, and Z. You, "Developments in ultrasonic modeling with finite element analysis," *J. Nondestruct. Eval.*, vol. 9, nos. 2–3, pp. 129–143, 1990.

[10] M. Rudolph, "Ultrasonic beam models in anisotropic media," Ph.D. dissertation, Iowa State Univ., Ames, IA, USA, 1999.

[11] B. E. Treeby and B. T. Cox, "A *k*-space Green's function solution for acoustic initial value problems in homogeneous media with power law absorption," *J. Acoust. Soc. Amer.*, vol. 129, no. 6, pp. 3652–3660, 2011.

[12] L. Demi, K. W. A. van Dongen, and M. D. Verweij, "A contrast source method for nonlinear acoustic wave fields in media with spatially inhomogeneous attenuation," *J. Acoust. Soc. Amer.*, vol. 129, no. 3, pp. 1221–1230, 2011.

[13] H. Jeong, D. Barnard, S. Cho, S. Zhang, and X. Li, "Receiver calibration and the nonlinearity parameter measurement of thick solid samples with diffraction and attenuation corrections," *Ultrasonics*, vol. 81, pp. 147–157, Nov. 2017.

[14] J. H. Cantrell, "Fundamentals and applications of nonlinear ultrasonic nondestructive evaluation," in *Ultrasonic Nondestructive Evaluation*, 1st ed. Boca Raton, FL, USA: CRC Press, 2003.

[15] Y. Ohara, K. Takahashi, Y. Ino, and K. Yamanaka, "Nonlinear ultrasonic phased array imaging of closed cracks using global pre-heating and local cooling," in *Proc. AIP Conf.*, vol. 1685, 2015, Art. no. 080002.

[16] Z. Zhou and S. Liu, "Nonlinear ultrasonic techniques used in nondestructive testing: A review," *J. Mech. Eng.*, vol. 47, no. 8, pp. 2–11, 2011.

[17] M. D. Verweij, L. Demi, and K. W. A. van Dongen, "Computation of nonlinear ultrasound fields using a linearized contrast source method," *J. Acoust. Soc. Amer.*, vol. 134, no. 2, pp. 1442–1453, 2013.

[18] R. B. Thompson and E. F. Lopes, "The effects of focusing and refraction on Gaussian ultrasonic beams," *J. Nondestruct. Eval.*, vol. 4, no. 2, pp. 107–123, 1984.

[19] J. J. Wen and M. A. Breazeale, "A diffraction beam field expressed as the superposition of Gaussian beams," *J. Acoust. Soc. Amer.*, vol. 83, no. 5, pp. 1752–1756, 1988.

[20] M. Spies, "Analytical methods for modeling of ultrasonic nondestructive testing of anisotropic media," *Ultrasonics*, vol. 42, nos. 1–9, pp. 213–219, 2004.

[21] R. Huang, "Ultrasonic modeling for complex geometries and materials," Ph.D. dissertation, Iowa State Univ., Ames, IA, USA, 2006.

[22] Z. Lu, C. Xu, D. Xiao, and F. Meng, "Nondestructive testing method for curved surfaces based on the multi-Gaussian beam model," *J. Nondestruct. Eval.*, vol. 34, no. 4, pp. 1–39, 2015.

[23] L. Azar, Y. Shi, and S.-C. Wooh, "Beam focusing behavior of linear phased arrays," *NDT E Int.*, vol. 33, no. 3, pp. 189–198, Apr. 2000.

[24] L. W. Schmerr, *Fundamentals of Ultrasonic Phased Arrays*, vol. 215. Cham, Switzerland: Springer, 2015.

[25] H. J. Kim, L. W. Schmerr, and A. Sedov, "Generation of the basis sets for multi-Gaussian ultrasonic beam models," in *Proc. AIP Conf.*, vol. 760, 2005, pp. 978–985.

[26] J. S. Park, S. J. Song, and H. J. Kim, "Calculation of radiation beam field from phased array ultrasonic transducers using expanded multi-Gaussian beam model," *Solid State Phenomena*, vol. 110, pp. 163–168, Mar. 2006.

[27] R. Huang, L. W. Schmerr, and A. Sedov, "Modeling the radiation of ultrasonic phased-array transducers with Gaussian beams," *IEEE Trans. Ultrason., Ferroelectr., Freq. Control*, vol. 55, no. 12, pp. 702–2692, Dec. 2008.

[28] H. Jeong and L. W. Schmerr, "Ultrasonic beam propagation in highly anisotropic materials simulated by multi-Gaussian beams," *J. Mech. Sci. Technol.*, vol. 21, no. 8, pp. 1184–1190, 2007.

[29] D. Ding, Y. Zhang, and J. Liu, "Some extensions of the Gaussian beam expansion: Radiation fields of the rectangular and the elliptical transducer," *J. Acoust. Soc. Amer.*, vol. 113, no. 6, pp. 3043–3048, 2003.

[30] V. Cerveny, *Seismic Ray Theory*. Cambridge, U.K.: Cambridge Univ. Press, 2001.

[31] X. Zhao and T. Gang, "Nonparaxial multi-Gaussian beam models and measurement models for phased array transducers," *Ultrasonics*, vol. 49, no. 1, pp. 30–126, 2009.

[32] *COMSOL Multiphysics 5.3 User's Guide Manual*, COMSOL BV, Zoetermeer, The Netherlands, 2014.

[33] B. P. Newberry and R. B. Thompson, "A paraxial theory for the propagation of ultrasonic beams in anisotropic solids," *J. Acoust. Soc. Amer.*, vol. 85, no. 6, pp. 2290–2300, 1989.

Chirag Anand was born in Mumbai, India, in 1988. He received the M.E. degree in aeronautical engineering from Anna University, Chennai, India, in 2011. He is currently pursuing the Ph.D. degree with the Faculty of Aerospace Engineering, Technical University of Delft, Delft, The Netherlands, with a focus on modeling of phased array inspection of anisotropic structures and imaging of composite materials using phased arrays.

His research interests include ultrasonic imaging using phased arrays, wave propagation, signal processing, and analytical and numerical modeling of ultrasonic non-destructive testing (NDT) for anisotropic materials.

Steven Delrue was born in Kortrijk, Belgium, in 1985. He received the M.Sc. degree in mathematics from KU Leuven, Leuven, Belgium, in 2007, and the Ph.D. degree in mathematical physics and applied mathematics from KU Leuven Kulak, Kortrijk, in 2011, with a focus on the development of numerical models to support and optimize experimental techniques for ultrasonic non-destructive testing.

Since 2011, he has been a Postdoctoral Lecturer with the Wave Propagation and Signal Processing Research Group, KU Leuven Kulak. His current research interests include the numerical modeling of contact defects and their interaction with ultrasonic waves, nonlinear signal processing techniques, ultrasonic thermography, and ultrasonic imaging using phased arrays.

Hyunjo Jeong was born in South Korea in 1958. He received the B.S. degree from Hanyang University, Seoul, South Korea, in 1980, and the M.S. degree from the Rensselaer Polytechnic Institute, Troy, USA, in 1986, all in mechanical engineering, and the Ph.D. degree in engineering mechanics from Iowa State University in 1990.

After working as a Post-Doctoral Associate with the CNDE, Iowa State University, he joined the Agency for Defense Development, South Korea, as a Senior Researcher. He was in charge of the design and NDI of composite structures. He has been an Assistant Professor of mechanical engineering with Pusan National University, South Korea, since 1996, and has been a Professor with Wonkwang University, Iksan, South Korea, since March 2000. His current research interests include nonlinear characterization of material properties, time reversal signal processing, and ultrasonic NDE. He is currently the Vice President of the Korean Society for Mechanical Technology and the Editor of the *Journal of the Korean Society for Nondestructive Testing* (KSNT).

Sonell Shroff was born in Kolkata, India, in 1984. She received the M.Sc. degree in aerospace engineering and the Ph.D. degree in aerospace structures and materials from the Delft University of Technology, Delft, The Netherlands, in 2009 and 2014, respectively.

She was an Assistant Professor with the Structural Integrity and Composites Group, Delft University of Technology, until 2018, where she specialized in automated production methods of composite materials for aerospace applications, with a keen interest in *in situ* consolidation of thermoplastic composites. Since May 2019, she has been a Project Officer at the Clean Sky 2 Joint Undertaking of the European Commission, Brussels, Belgium. Her work in design, analysis, fabrication, and testing of grid-stiffened structures in fuselage applications was published in a series of journal articles and the technology developed for manufacturing and testing is widely used in research and small-scale prototyping environments in aerospace and wind energy alike.

Roger M. Groves received the B.Sc. degree in chemistry, the M.Sc. degree in applied physics, and the Ph.D. degree in optical instrumentation from Cranfield University, Bedford, U.K., in 1988, 1997, and 2002, respectively.

He was a Senior Scientist with the Institute for Applied Optics (ITO), University of Stuttgart, Stuttgart, Germany. In 2008, he joined Delft University of Technology (TU Delft), Delft, The Netherlands, as an Assistant Professor to set up a new research activity in non-destructive testing (NDT)/structural health monitoring (SHM). This research activity has grown to 20 persons and is active in research in optical metrology, fiber-optic sensing, and ultrasonics for aerospace and cultural heritage applications. He is currently an Associate Professor in aerospace NDT/SHM and heritage diagnostics with TU Delft. He has over 150 journal and conference publications in this field.

Rinze Benedictus received the Ph.D. degree in metallurgy from the University of Delft, Delft, The Netherlands, in 1997, with a focus on metallic multilayers. He studied applied physics at the University of Groningen, Groningen, The Netherlands, where he specialized in the physics of thin layers.

He is currently a Professor of structural integrity and composites with the Technical University of Delft, where he is also the Head of the Department of Materials, Structures and Mechanics and the Vice-Dean of the Faculty of Aerospace Engineering. He is also a Board Member of the Fibre Metal Laminate Centre (FMLC) and the Hechtingsinstituut (Adhesion Institute) and a Scientific Advisor of the Dutch National Aerospace Laboratory (NLR) and the Ministry of Economic Affairs with respect to the program on self-healing materials. He has published over 60 journal articles in different fields of physics, materials science, and aerospace engineering. He has over 50 patents assigned to his name. The current research within the chair exploits the potential synergy between materials and structure in advancing the performance and capabilities of the aerospace products of tomorrow. The focus is on structural integrity. The main topics are damage-tolerant concepts for composite structures and fiber metal laminates, manufacturing, and non-destructive testing.